Since January 2020 Elsevier has created a COVID-19 resource centre with free information in English and Mandarin on the novel coronavirus COVID-19. The COVID-19 resource centre is hosted on Elsevier Connect, the company's public news and information website.

Building and Environment 99 (2016) 13–21

Contents lists available at ScienceDirect

Building and Environment

journal homepage: www.elsevier.com/locate/buildenv

On-site measurement of tracer gas transmission between horizontal adjacent flats in residential building and cross-infection risk assessment

Yan Wu, Thomas C.W. Tung, Jian-lei Niu*

Department of Building Services Engineering, The Hong Kong Polytechnic University, Hunghom, Kowloon, Hong Kong

ARTICLE INFO

Article history:
Received 10 November 2015
Received in revised form
4 January 2016
Accepted 16 January 2016
Available online 18 January 2016

Keywords:
Airborne transmission
Infection risk
On-site measurement
Tracer gas
Air infiltration
Residential building

ABSTRACT

Airborne transmission is a main spread mode of respiratory infectious diseases, whose frequent epidemic has brought serious social burden. Identifying possible routes of the airborne transmission and predicting the potential infection risk are meaningful for infectious disease control. In the present study, an internal spread route between horizontal adjacent flats induced by air infiltration was investigated. On-site measurements were conducted, and tracer gas technique was employed. Two measurement scenarios, closed window mode and open window mode, were compared. Using the calculated air change rate and mass fraction, the cross-infection risk was estimated using the Wells–Riley model. It found that tracer gas concentrations in receptor rooms are one order lower than the source room, and the infection risks are also one order lower. Opening windows results in larger air change rate on the one hand, but higher mass fraction on the other hand. Higher mass fraction not necessarily results in higher infection risk as the pathogen concentration in the source room is reduced by the higher air change rate. In the present study, opening windows could significantly reduce the infection risk of the index room but slightly reduce the risks in receptor rooms. The mass fraction of air originated from the index room to the receptor units could be 0.28 and the relative cross-infection risk through the internal transmission route could be 9%, which are higher than the external spread through single-sided window flush. The study implicates that the horizontal transmission route induced by air infiltration should not be underestimated.

1. Introduction

In recent years, frequent outbreaks of infectious diseases have threatened public health, such as the recently epidemic Middle East Respiratory Syndrome (MERS) in 2015, Ebola Virus Disease (EVD) in 2014, Influenza A virus subtype H7N9 in 2013, H1N1 in 2009 and Severe Acute Respiratory Syndrome (SARS) in 2003. The main spread modes of infectious diseases are direct contact transmission, large droplet contact transmission and airborne transmission. Airborne transmission has been supposed to be responsible for the spread of many respiratory infectious diseases, such as tuberculosis, measles, influenza, smallpox and SARS [1–3]. Riley et al. [4] implicated the ventilation system with a measles epidemic in a school in 1974, in which 60 children were infected. Yu and Li et al. [5,6] associated the not uniformed distribution of infected cases in the Amoy Gardens housing during 2003 SARS epidemic with the dispersion of airborne aerosols predicted using the computational fluid dynamics and multi-zone modeling. It found that the risk distribution characteristics, upper floors had higher risks than lower floors, matched with the rising plume in the airshaft, and the hypothesis of the airborne spread of virus-laden aerosols was also identified. Therefore, airborne transmission should not be underestimated [7]. The airborne spread of virus is within short-distance due to the interaction of respiration. However, relying on air movement, it might be long-distance spread and could contribute to large-scaled outbreaks of infectious diseases [8]. Research showed that the dispersion of aerosols could even be over 6 km [9]. Exploring the possible airborne transmission routes related to air movement and assessing the infection risk seems to be essential for the control of infectious diseases. Many works on airflow and dispersion have been done, which enhanced the confidence to

* Corresponding author.
E-mail address: bejlniu@polyu.edu.hk (J.-l. Niu).

http://dx.doi.org/10.1016/j.buildenv.2016.01.013
0360-1323/

investigate the air movement induced contaminant dispersion [10–13]. In hospital environment or enclosed environment like aircraft cabin, relevant guidelines have been raised [14–16]. The influences of mechanical ventilation, human walking and door motion on the airborne transmission have been well analyzed. Improved ventilation design for isolation rooms was recommended, which can be considered an improvement of the previous ventilation strategy proposed by Centers for Disease Control and Prevention. Besides, potential inter-cubicle transmission was also explored and related solutions to reduce inter-cubicle exposure hazards were put forward [17–20]. However, in densely populated residential environment, there is still a lack of the understanding of, the risk level and mechanism of possible airborne spread routes.

An external spread route, that the air exhausts from the windows of the lower floor and re-enters the upper floor, has been identified, which is induced by single-sided natural ventilation. Niu and Tung's on-site measurements in a multi-family residential building revealed that the upper floor inhales up to 7% of exhaust air from the low floor [21]. Gao et al. [22,23] further studied this spread route using numerical methods. Both the dispersions of the tracer gas and the particle were simulated. It found that the tracer gas concentration in upper floor is two orders lower than that in the immediate lower source floor, while particle concentration is two to three orders lower than the source floor. The infection risk in upper floor is one order lower than in the lower source floor. Outdoor wind normal to the building may restrain or reinforce the upward dispersion depending on the wind speed magnitudes. Liu et al. [24,25] investigated the tracer gas dispersion and cross-contamination through the external route by conducting wind tunnel tests, and found that not only the vertical upward but also vertical downward and horizontal transmission were observed under wind effects. Ai et al. [26–29] optimized the numerical methods for the simulations of the single-sided ventilation induced inter-unit dispersion, including the employment of inhomogeneous atmospheric boundary layer, the treatment of near-wall simulation and the methods for the determination of sing-sided ventilation rates. It is found that the inter-unit reentry ratios could reach around 10.0%, and that the building envelope features could affect the gaseous dispersion. The strongest dispersion occurs on the windward wall of the buildings due to high air change rate. However, these studies only focused on the transmission through external routes of buildings with single-sided ventilation. Other transmission routes intra a multiunit residential building could also be possible.

In the present study, a possible internal transmission route between horizontal adjacent flats induced by air infiltration was investigated. Many works about the infiltration have been conducted, but they mainly concentrated on the determination of the infiltration flow rate and its impact factors [30,31]. Research that associates the air infiltration with the contaminants transmission was limited. In the present study, on-site measurements were carried out, and tracer gas technique was employed to simulate the diffusion of gaseous pollutants or fine particles. Although the transport of coarse particles could be significantly limited by the deposition and gravitational effects, fine particles less than 1.0 μm disperse like gaseous pollutants [23]. Zhao and Wu [32] compared the diffusion of particles in size range 0.3–20 μm with passive pollutants, and found that, when the indicator, the product of the nominal time and the particle relaxation time, is small enough, particles could be treated as gaseous pollutants. The main objectives of this study are to verify the internal transmission route and to assess the relative cross-infection risks of this route.

2. Methodology

2.1. Measurement settings and instrumentations

On-site measurements were carried out in a slab-type building located in Pak Tin Estate, Hong Kong, which is a 16-story public housing built in 1979. Subject to the complicated mountainous terrain in Hong Kong, many different designs were used in building constructions, such as slab type, H type, tower type, I type, harmony type, linear type, trident type, mark type, cruciform type, concord type and so on. Among them, slab-type housing is one of the most common and basic designs, especially in public housing estates, which provide houses for more than 30% populations in Hong Kong. Besides, slab-type design is also widely used in the buildings of hospital wards and student dormitories. The typical building plan of the test housing is shown in Fig. 1. In each floor, there are 40 flats, with 20 in each side of a 1.75 m width corridor. At both ends of the corridor, there are windows opened most of the time. Three horizontal adjacent flats in 13th floor were rented for the measurements with two flats (R1308 and R1310) in the west side and another one (R1307) in the east side opposite to R1308. The interior structures in a unit are shown in Fig. 2. In each unit, there is a living room near the corridor and a lavatory and a kitchen on the balcony. Between the living room and the balcony, there is a partition containing a door and a window, which could be fully closed. On the internal walls near the corridor, windows are designed, which are closed in most cases for privacy reason. In the present measurements, gaps have to be left on the internal windows for the arrangement of the tracer gas sampling tubes. On the external wall of each unit, windows and air slits are designed for natural ventilation.

The measurements last for three months from March to May 2015. Two measurement scenarios were carried out. Scenario 1 is closed window mode (simplified as Close mode below), which was carried out in March and April, and Scenario 2 is open window mode (simplified as Open mode) conducted in the end of April and May. In Close mode, all the doors, including the entrance doors, kitchen doors, lavatory doors and the doors on the partitions that connect the living rooms and the balconies, and all the windows, including internal windows, partition windows and external windows, in three flats were closed. The setting of closed windows is in conformity with the occupant behavior in cool season. The tracer gas dispersion is mainly induced by the infiltration flow through cracks of building components. The dimensions of cracks were measured, which are 0.5~2 cm width on doors, and 1~2 cm and 2~3 cm width for external and internal windows. The effective air leakage areas for doors and windows are about 360 cm^2/ea and 120 cm^2/m^2, respectively. They are much larger than the values in ASHRAE Handbook, in which the best estimated effective air leakage areas for residential entrance doors, internal doors and windows are 70 cm^2/ea, 21 cm^2/ea and 1.6 cm^2/m^2, respectively. In Open mode, the windows on external facades and on the partitions were open at an angle of 45°, while the internal windows towards the corridor and all the doors were closed. The setting of open external windows conforms to the occupant behavior in warm seasons. In this scenario, with the influence of natural ventilation near building facades, the pressure difference that drives the infiltration flow and dispersion between units would increase. Besides, it should be mentioned that during the test period there were residents in other flats on the same floor, and their living behaviors were not controlled. Whether their external windows were closed or open may also affect the airflow and dispersion in the common corridor.

In the measurements, the tracer gas technique was used to identify the indoor airflow pattern and to reproduce the pathogens

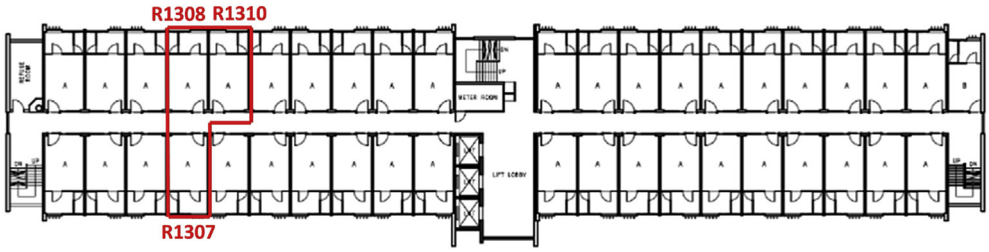

Fig. 1. Schematic diagram of the building plan and location of rented flats.

(a) The partition between the living room and the balcony

(b) The window on the internal wall near the corridor

(c) The window and air slits on the external wall

Fig. 2. Building structures in the flats. (a) The partition between the living room and the balcony. (b) The window on the internal wall near the corridor. (c) The window and air slits on the external wall.

dispersion. SF_6 (Sulfur hexafluoride) and CO_2 (Carbon dioxide) were provided as tracers. Both of them were used at low concentrations that are known to be not harmful to the residents. SF_6 was tracer for pollutant dispersion analysis and ventilation rate calculation, while the monitored CO_2 concentrations were used to calculate the ventilation rates based on tracer decay method. B&K Multi-gas Monitor 1302 and B&K Multipoint Sampler and Doser 1303 were used for SF_6 dosing and sampling in three flats. The CO_2 concentrations were monitored in three flats using 2 sets of TSI Q-Trak and 1 set of Telaire CO_2 Sensor. The wind speed condition was also measured, by locating a set of Young UVW Anemometers above the roof.

The distribution of SF_6 dosing and sampling points is shown in Fig. 3. The dosing point of SF_6 was set in R1307, the southeast flat among three rented flats, since that the dominant wind direction near the site is southeast according to the record of the Hong Kong Observatory in the last three years. 6 sampling points were distributed in three flats with two points in each flat, one in the center of the room (P-1, P-4 and P-6) and the other one in the crack of the internal window (P-2, P-3 and P-5). Before the startup of the measurement, the windows and doors of the flats were opened, and the outdoor fresh air was allowed to purge the old air out. Then the windows were closed or opened based on different scenarios to start the tracer gas release. SF_6 was injected to the dosing point with a constant rate of 3 ml/s. Air samples were extracted from 6 sampling points were analyzed in sequence, and the time taken to analyze 6 samples was about 5 min. CO_2 was released in three flats twice in a day to raise the indoor CO_2 concentrations above 2000 ppm. The first release was in the morning, and the second in the afternoon. The CO_2 concentration was monitored continuously and recorded once a minute. In these measurements, SF_6 was used both as the tracer of indoor gaseous pollutant and for the air change rate assessment. CO_2 was used as a double check of the air change rate. In addition, as SF_6 was released in the source/index room at a constant rate, to measure the air change rate in the other two adjacent rooms, a second tracer gas was needed. To assure better accuracy, the CO_2 concentrations were monitored continuously in the empty rooms, and the equilibrium CO_2 concentrations before and after each of the short dosing and decay period were good indictors of the real-time background concentration. Furthermore,

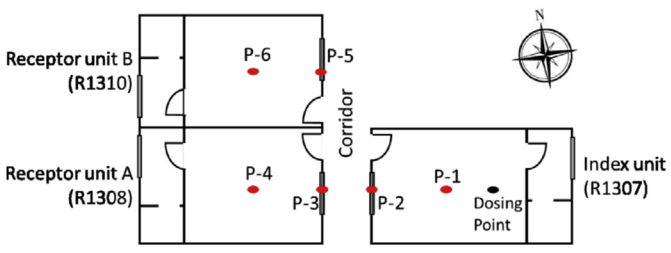

Fig. 3. Schematic locations of SF_6 dosing and sampling points.

the *ACH* obtained using the CO_2 decay method could be representative of the average *ACH* during the two short periods of CO_2 decay test on each day, which provides additional information on the possible variation of the air change.

During the test period of the Close mode, the outdoor temperatures were 20–28 °C, while they were 28–31 °C during the Open mode tests. But, considering that no occupant is allowed to stay and no air conditioning services were provided in all the test flats during tests, the indoor–outdoor temperature differences were quite small in the duration of measurement. The incoming wind conditions during the measurement periods for the two scenarios are shown in Fig. 4. It can be seen that the wind conditons were similar for the two scenarios. The wind speeds were mainly below 2 m/s, which were low-wind conditions.

2.2. Data analysis approach

To determine the air change rate of the index unit, the monitored SF_6 concentrations were employed. Assuming the steady airflow and well-mixed indoor tracer gas, the variation of SF_6 concentration against time can be calculated by the mass balance equation:

$$V\frac{dC}{dt} = E + Q_0C_0 - QC \tag{1}$$

where, C is the indoor SF_6 concentration. C_0 is the SF_6 concentration in ambient fresh air, which equals to 0. V is the volume of the room. E is the known SF_6 emission rate, 3 ml/s Q_0 and Q are inflow rate from outdoor fresh air and outflow rate, respectively. For incompressible flow, $Q_0 = Q$. With the boundary conditions, t=0, C=C_i and $\frac{dC}{dt} = 0$, $C = C_\infty = \frac{E}{Q}$, the differential Equation (1) can be solved as the expression:

$$C = \left(C_i - \frac{E}{Q}\right)e^{\frac{-Qt}{V}} + \frac{E}{Q} \tag{2}$$

where, C_i is the initial SF_6 concentration, which can be obtained from the measurement data. C_∞ is the equilibrium SF_6 concentration. The well-mixed hypothesis could be verified with the measurement results in the following chapters, in which it is found that SF_6 concentration profiles of two sampling points in a some receptor flat seems to be similar, and their mean values are almost the same. Besides, considering that the measurements were carried out in empty rooms, and the tracer gases employed are chemically stable, the sink effects were ignored in the mass balance formulas above.

By minimizing the sum deviation between measured SF_6 concentration data and theoretical calculated data by Equation (2), the air flow rate Q could be obtained using the statistic approach of least square fitting [33]. Accordingly, the equilibrium SF_6 concentration C_∞ could also be calculated. In reality, the monitored SF_6 concentration changed all the time, and the air flow rate was also variable. Therefore, the constant values of Q and C_∞ achieved from theoretical fitting only reflect the equivalent air flow rate and corresponding indoor tracer gas level. Measured and fitted SF_6 variation curves of a test day in the index room is provided as an example in Fig. 5. As an important parameter to assess the infection risks, the equivalent air change rate Q of the index room, was obtained not only from the SF_6 variation, but also from the well-estimated CO_2 concentration decay method [34–36], as illustrated in Fig. 6. The differences of the air flow rates calculated by using the SF_6 constant realease method and CO_2 decay method are below 35% for the Close mode and below 21% for the Open mode. For the receptor units, R1308 and R1310, air change rates were calculated using the CO_2 decay method, as the tracer gas SF_6 was realeased in the source room.

To assess the infection risk of diseases, an index, infection probability P, is calculated using the Wells–Riley model [4]. The Wells–Riley model is proposed based on the hypothesis of the quantum of infection, which is the number of infectious pathogens required to infect people, and developed by considering the inhaled dose of pathogens. It has been extensively applied for infection risk assessment, especially for airborne transmission infectious diseases [37,38]. The Wells–Riley equation was shown as follows:

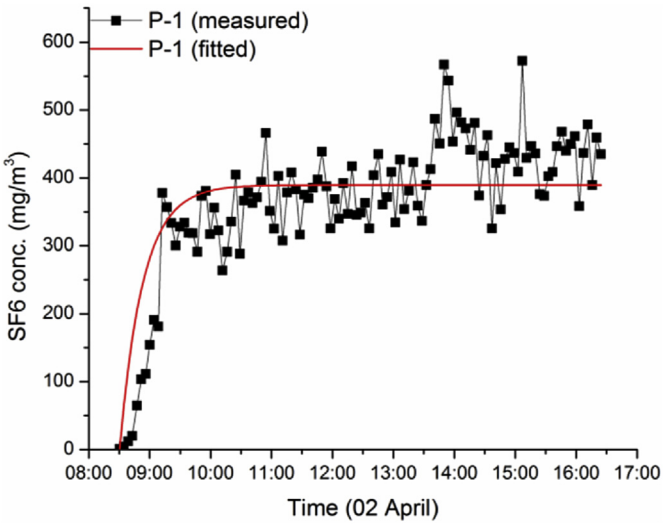

Fig. 5. Measured and fitted SF_6 concentration against time in the index room.

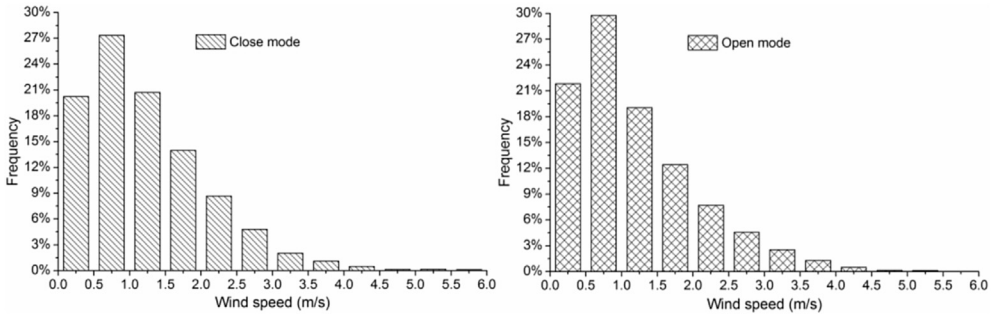

Fig. 4. Wind frequency during the test periods for two scenarios.

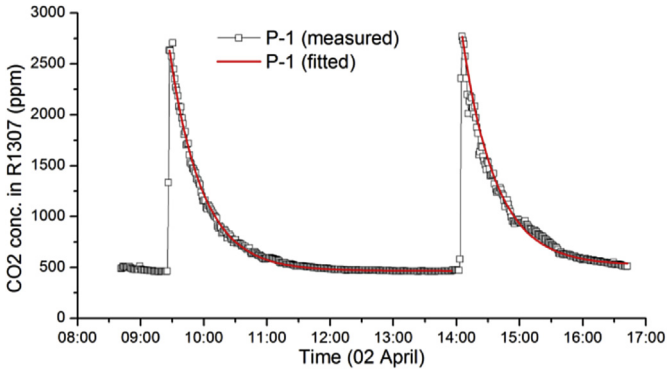

Fig. 6. Measured and fitted CO_2 concentration against time in the index room.

$$P = 1 - e^{\frac{-IqptV}{Q}} \quad (3)$$

where, q is the quanta generation rate, which is the infectious source strength term considering both the emission rate and the infectivity of the pathogen [39]. I is the number of infectors, p is the pulmonary ventilation rate of a person, t is the exposure time, Q is the air flow rate, V is the room volume. To predict the infection risk of a specific disease, the values of quanta generation rate q, pulmonary ventilation rate p and exposure time t could be obtained epidemiologically from an outbreak case with known attack rate. In the present study, these parameters are set same with our previous study about the vertical dispersion [22] for the comparison between two transmission routes. Where, infector number in the index room is 1, the quanta generation rate is 13 quanta per hour (q = 13), the pulmonary ventilation rate of a person is 0.6 m^3/h (p = 0.6), and the exposure time is 8 h (t = 8). To predict the infection risk in the index room using Equation (3), the air change rate Q/V found from on-site measurements is also required. It should be noticed that since the air change rate used was the equivalent value which was obtained under the steady airflow assumption, the peak risk under the worst condition may be underestimated. Besides, the calculated infection risks here are relative values rather than absolute risks.

For the receptor rooms, it is the pathogens originating from the index room that could cause illness. To assess the cross-infection risks in receptor rooms, the quanta concentration in the receptor units should be $\frac{-IqMV}{Q}$ rather than $\frac{-IqV}{Q}$. Where, the mass fraction M_{i-j}, was defined as the fraction of air in the point j that stems from the point i, which was obtained directly using the equilibrium tracer gas concentrations as follows:

$$M_{i-j} = \frac{C_{\infty j}}{C_{\infty i}} \quad (4)$$

In the present study, $M_{1\text{-}4}$ and $M_{1\text{-}6}$ were calculated to reflect the tracer gas transmission level from the index room to two receptor rooms, respectively. With the mass fraction M and air change rate of the index room Q/V obtained from the on-site monitoring, the cross-infection risks of receptor rooms could be calculated with the equation as follows:

$$P = 1 - e^{\frac{-IqptMV}{Q}} \quad (5)$$

3. Results and discussion

3.1. Tracer gas dispersion characteristics and incoming wind condition

The monitored SF_6 concentrations and incoming wind of several test days are shown in Fig. 7 and Fig. 8. The SF_6 concentrations of 6 sampling points are presented in logarithmic scale. The locations of the points were illustrated in Fig. 3. The wind speeds are reported as vector components, in which U+ is in east direction, V+ is north and W+ is upward.

For both closed window and open window scenarios, the SF_6 concentrations in receptor rooms are about one order lower than that in the index room. For the Close mode, the SF_6 concentrations decrease gradually, from P-1 to P-6. It is to say, the transmission route of the tracer gas from the index room to receptor rooms is across the internal window leakage and the corridor. Along the routes, Point 1-2-3-4, and Point 1-2-5-6, tracer gas dilutes, especially while passing through the corridor. Comparing the tracer gas concentrations at two sampling points in a same room, it can be observed that points in the window cracks have more fluctuant concentrations than the points in the room centers. This may have been caused by the frequent switch of airflow directions through the cracks. Besides, the SF_6 concentrations at P-3 and P-4 in the closer receptor room A are higher than those at P-5 and P-6 in the

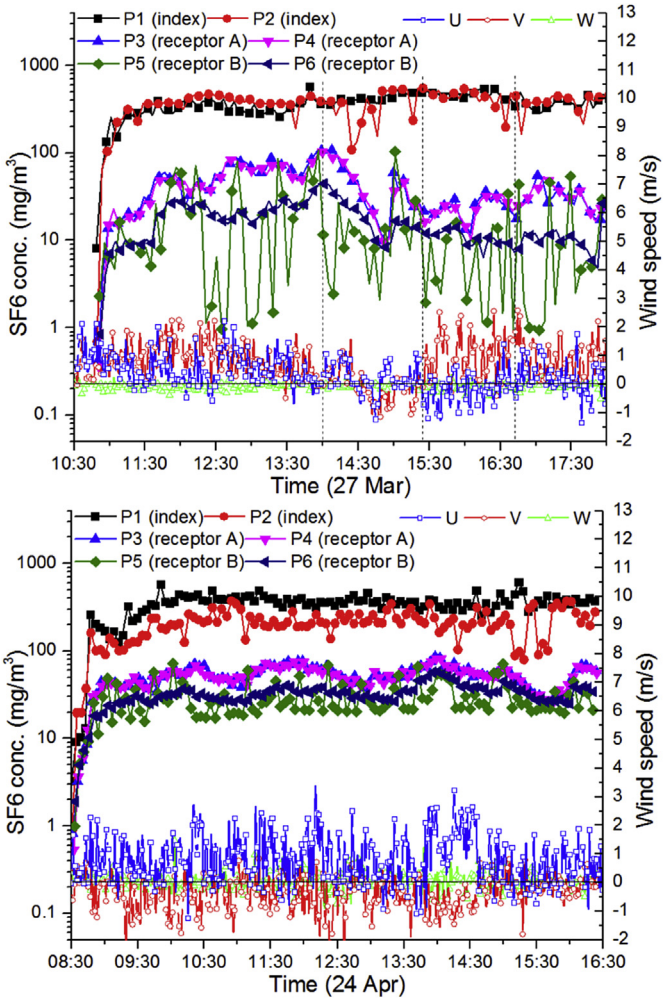

Fig. 7. SF_6 concentration profiles and wind profiles for the Close mode.

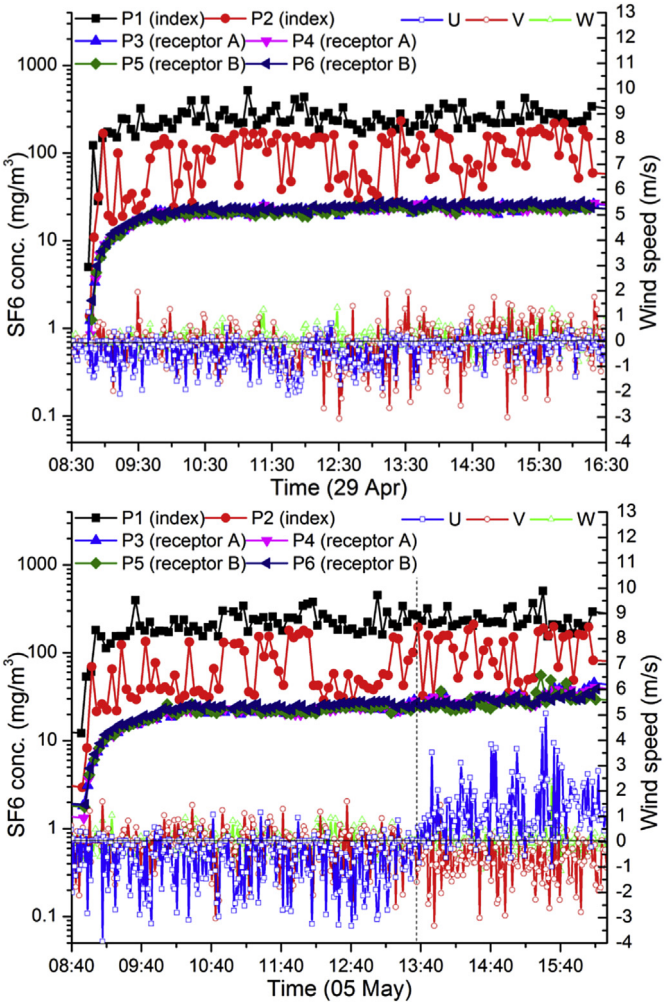

Fig. 8. SF_6 concentration profiles and wind profiles for the Open mode.

farther receptor room B. With the increase of the distance between the sampling point and dosing point, the concentration decreases. However, for the Open mode, SF_6 concentrations in the two receptor rooms are almost the same. It indicates that as the windows are open, the tracer gas was well mixed to the same concentration level in the corridor, at least in the region near the two receptor rooms.

The influence of the wind condition on the tracer gas transmission could be recognized especially for the Close mode. From the profiles of 27 March (Fig. 7), it can be seen that SF_6 concentrations in the receptor rooms during the period of 15:30–16:30 were relatively lower than other periods due to the negative U component of wind speed. Besides, the remarkable variations of tracer gas concentrations in receptor rooms during 14:00–15:30 were also consistent with the fluctuations of U wind component. Moreover, the fluctuations of the SF_6 concentration in the receptor rooms on 27 March were much more drastic than other days, which may be attributed to the frequent shift of wind directions observed on that day. For the Open mode, the wind fluctuation induced concentrations variations were much weaker except at P-2, the sampling point in the window crack of the index room. However, the concentration fluctuations seem not as tied to the fluctuations of the incoming wind. With the irregular fluctuation of the incoming wind condition, the effective tracer gas transmission is extremely complicated, which will be further explored separately.

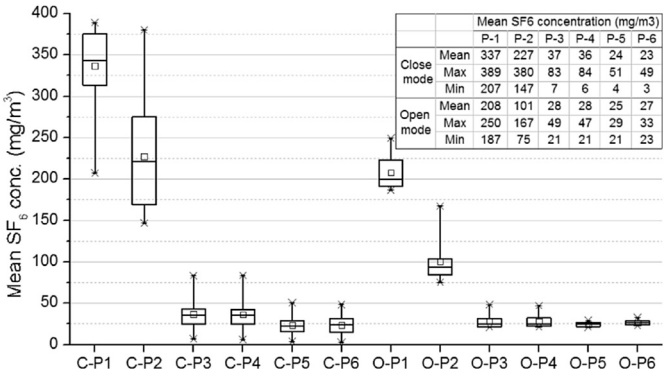

Fig. 9. Box charts of the mean SF_6 concentrations (C for Closed window mode, O for Open window mode, P1~P6 are the sampling points).

The mean SF_6 concentration at each sampling point on each test day was calculated for both scenarios. The statistic results for the whole monitoring period are shown in Fig. 9. The box ranges from 25th to 75th percentiles with a line in the box reflects 50th percentiles of a data group. Inside the box, the small square symbol "□" indicates the mean value of the data group. And the cross symbols "×" at the top and bottom of the whisker show the maximum and minimum values, respectively. It can be observed that tracer gas concentration levels in the receptor rooms are one order lower than that in the index room for both closed and open window mode. The mean SF_6 concentrations in the index room are 337 mg/m^3 and 208 mg/m^3, respectively for the closed window and open window conditions. The former one is much higher. For the Close mode, the mean SF_6 concentrations in the two receptor rooms are different, with values of 36 mg/m^3 for the closer one and 23 mg/m^3 for the furthur one, respectively, while for the Open mode they are the same with the mean value of around 28 mg/m^3. Besides, the longer whiskers of the box charts for the Close mode indicates that the tracer gas concentration levels are more variable. For both conditions, the tracer gas concentrations at the two sampling points in the same receptor room are fairly close, though concentrations at the window cracks fluctuate more drastically than those in the room centers. It indicates that tracer gas in the two receptor rooms tend to be well-mixed.

3.2. Cross-infection risk assessment

With the monitored SF_6 and CO_2 concentration data, the air change rate, mass fraction and relative infection risk of each test

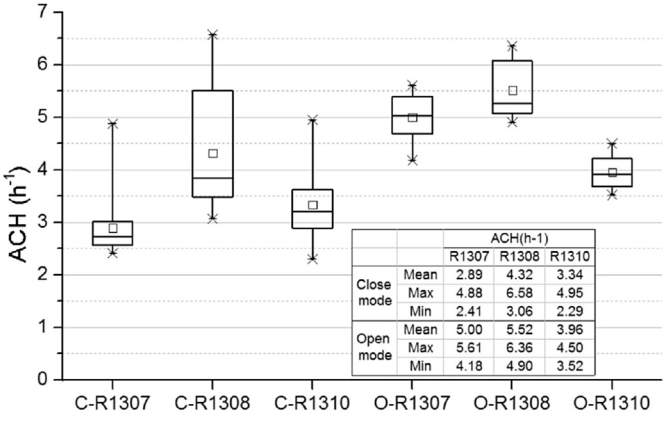

Fig. 10. Air change rate for both scenarios (C for Closed window mode, O for Open window mode, R1307 is the index room, R1308 and R1310 are the receptor rooms).

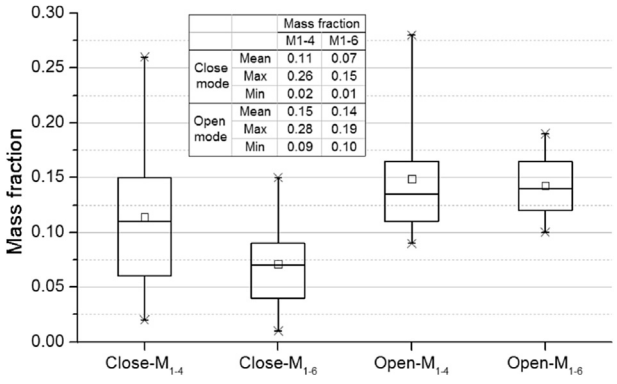

		Mass fraction	
		M1-4	M1-6
Close mode	Mean	0.11	0.07
	Max	0.26	0.15
	Min	0.02	0.01
Open mode	Mean	0.15	0.14
	Max	0.28	0.19
	Min	0.09	0.10

Fig. 11. Mass fraction for both scenarios.

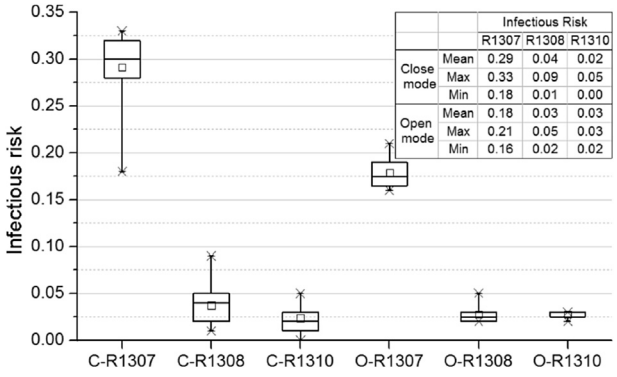

		Infectious Risk		
		R1307	R1308	R1310
Close mode	Mean	0.29	0.04	0.02
	Max	0.33	0.09	0.05
	Min	0.18	0.01	0.00
Open mode	Mean	0.18	0.03	0.03
	Max	0.21	0.05	0.03
	Min	0.16	0.02	0.02

Fig. 12. Infection risk for both scenarios (C for Closed window mode, O for Open window mode, R1307 is the index room, R1308 and R1310 are receptor rooms).

day were calculated using the data analysis method introduced above. The statistic results for the whole monitoring period are shown in box charts in Fig. 10, Fig. 11 and Fig. 12. It can be seen that air change rate per hour (*ACH*) for the Open mode is significantly higher than that at the Close mode. Specifically, the mean *ACH* of the index room was below 3 at the Close mode, while it was 5 at the Open mode. It should be noted that 3 *ACH* under the closed window condition is still much higher than the recommended value of air leakage under 0.7–0.8 *ACH* for energy saving on the ASHRAE handbook. As a main factor that affects the infection risk, the higher *ACH* of the index room could effectively reduce the pathogen concentration in the index room and accordingly reduce the risk of infection.

Mass fraction is an important index that reflects the airborne transmission level. $M_{1\text{-}4}$ means mass fraction of air originating from P-1 in the index room and present at P-4 in the receptor room A. And $M_{1\text{-}6}$ is the mass fraction of air spreading from P-1 to P-6. For the Close mode the mass fractions in two receptor rooms are different, and for the Open mode they are almost the same. The mass fractions at the Open mode are higher than those at the Closed mode. The mean values of $M_{1\text{-}4}$ and $M_{1\text{-}6}$ are 0.11 and 0.07 when windows are closed. While they both rose to 0.15 as windows are open. The maximum value of mass fraction for the Open mode is 0.28, which is a little higher than the Close mode. That is to say, as the windows are open, more air from the index room flows into receptor units. However, subject to the relatively higher airflow rate as the windows were open, the tracer gas in the index room is more diluted and has lower concentration. Therefore, higher mass fraction not necessarily results in higher infection risk. While the cross-household infection risk is concerned, both the mass fraction

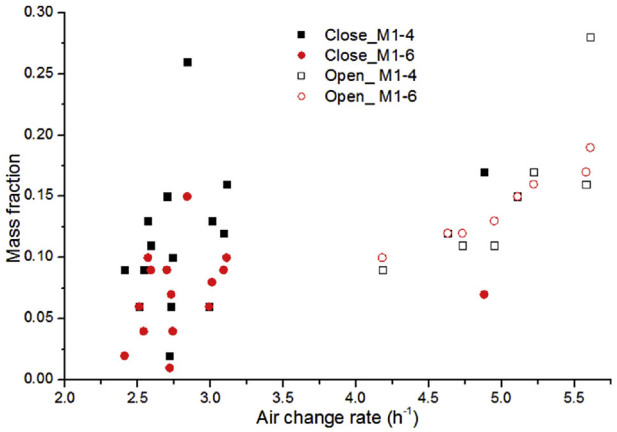

Fig. 13. Relationship between the air change rate and the mass fraction.

between the rooms and the pathogen concentration in the source room should to be considered, using Equation (7).

The estimated infection risks are shown in Fig. 12, it can be seen that in the index room, there is no doubt that opening the window could effectively reduce the risk of infection. For the Closed mode the maximum and mean infection risk of the index room are 0.33 and 0.29, while for the Open mode they are just 0.21 and 0.18. The infection risk in the index room is lower by one-third at the open window conditions. The mean infection risks in receptor rooms are one order lower than that in the index room. The mean cross-infection risks of the two receptor rooms are 0.04 and 0.02 for the Close mode, and 0.03 for the Open mode. The mean cross-infection risk levels are similar for both open window and closed window conditions, which indicates that opening windows did not effectively reduce the infection risks in the receptor room, since it increased the mass fraction and reduced the tracer gas concentration in the index unit at the same time. But, for the Closed mode, the maximum risk in the room R1308 is 0.09, while it is just 0.05 for the Open mode. It is to say, the maximum risk levels for the closed window mode is higher than the open window mode. It should be noted that the corridor in the present measurement has openings on both ends, which increases the airflow and helps to dilute the tracer gas spilled from the index room. In residential buildings with a sealed corridor space, the horizontal cross-infection risk could be higher.

The correlations of the three index, air change rate, mass

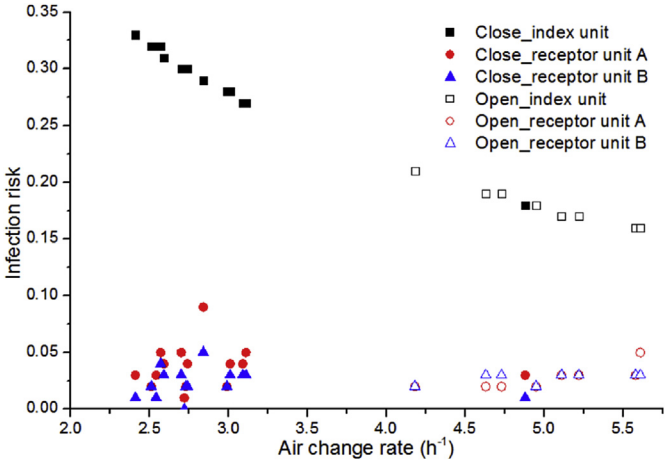

Fig. 14. Relationship between the air change rate and the infection risks.

Table 1
Correlations of air change rate with mass fraction and infection risk for the close mode.

		Mass fraction $M_{1\text{-}4}$	Mass fraction $M_{1\text{-}6}$	Risk of index unit	Risk of receptor unit A	Risk of receptor unit B
ACH of index unit (Close mode)	Correlation	0.350	0.138	−0.984**	−0.018	−0.149
	Sig. (2-tailed)	0.200	0.625	0.000	0.948	0.597
	N	15	15	15	15	15
ACH of index unit (Open mode)	Correlation	0.798*	0.971**	−0.989**	−0.776*	0.554
	Sig. (2-tailed)	0.018	0.000	0.000	0.024	0.154
	N	8	8	8	8	8

* Correlation is significant at the 0.05 level (2-tailed).
** Correlation is significant at the 0.01 level (2-tailed).

fraction and infection risk, were summarized in Fig. 13, Fig. 14 and Table 1. It found that when the windows are closed, *ACH* is mainly between 2.25 and 3.25 h^{-1}. While it is between 4 and 5.5 h^{-1} as the windows are open. *ACH* is positively correlative with the mass fraction especially for the open mode. The infection risk of the index unit is negatively related to the *ACH*, while in receptor units their correlations are not significant.

Compared with our previous study on the vertical transmission through the open windows flush induced by the single-sided natural ventilation [21,22], in which the maximum value of infection probability is 6.6% and the maximum mass fraction is below 0.09, the cross-infection risk via the internal horizontal spread route induced by air leakage in the present study is higher with a maximum infection risk of 9% and maximum mass fraction of 0.28. It should be noted that in all above studies, tracer gas was used to explore possible airborne transmission route. Tracer gas could pass through cracks on building envelopes without absorption, but particles may not [40]. Particles of 0.02–7 μm could completely penetrate through building envelopes when the cracks are larger than 1 mm and the pressure difference are higher than 4 Pa [41]. But under the experimental conditions of Tung et al.'s study, 15–30% of particle in the size range of 0.43–10 μm could be trapped by the building shell [42]. Besides, the particle deposition onto indoor surfaces can also limit the spread [43]. Therefore, the cross-contaminate risk in the present study may be over-estimated.

4. Conclusions

On-site measurement was carried out to explore possible airborne transmission route in a slab-type building. The tracer gas concentrations in three horizontal adjacent flats were monitored. The mean daily air change rates were obtained by both SF_6 constant release and CO_2 decay methods, and the inter-household air transmission was quantified using the mass fraction index. The relative risks of infection were assessed using Wells–Riley model. It is found that, the internal spread route between horizontal adjacent flats induced by air infiltration could be verified. The tracer gas concentrations in the receptor rooms are one order lower than that in the index room, and the relative risks are also one order lower in terms the infection probability. In general, with the open external windows, larger air change rate would reduce the airborne infection risks within the infector room. While opening external windows does not significantly reduce the cross infection risks in the receptor units. This is because there is a simultaneous increase of the mass fraction together with the dilution of the pathogens in the infector room. It should be cautioned that this conclusion is based upon the specific wind conditions during the late spring and early summer season in Hong Kong, and specific building configuration investigated. The cross-infection risk through this air infiltration induced spread route could be up to 9%, which is higher than the risk of 6.6% occurred via the vertical spread route through the single-sided open windows. Also the risk assessment is done using the Wells–Riley model, which was originally developed for well-mixed single space condition. With infiltration flow through window and door gaps, the aerosol state pathogens may deposit with a significant portion, therefore the risk probability would be lower, but on the other hand, the exposure time is assumed to be 8 h, which can vary quite widely in the residential environment.

Acknowledgment

The research is financially funded by Health and Medical Research Fund, Hong Kong SAR Government, with the project reference no.13121442. The authors would like to thank Hong Kong Housing Department and Hong Kong Housing Authority for providing the flats for the on-site measurements.

References

[1] M. Nicas, W.W. Nazaroff, A. Hubbard, Toward understanding the risk of secondary airborne infection: emission of respirable pathogens, J. Occup. Environ. Hyg. 2 (2005) 143–154.
[2] R.L. Riley, Airborne infection, Am. J. Med. 57 (1974) 466–475.
[3] Y. Li, G. Leung, J. Tang, X. Yang, C. Chao, J. Lin, et al., Role of ventilation in airborne transmission of infectious agents in the built environment–a multidisciplinary systematic review, Indoor air 17 (2007) 2–18.
[4] E. Riley, G. Murphy, R. Riley, Airborne spread of measles in a suburban elementary school, Am. J. Epidemiol. 107 (1978) 421–432.
[5] I.T. Yu, Y. Li, T.W. Wong, W. Tam, A.T. Chan, J.H. Lee, et al., Evidence of airborne transmission of the severe acute respiratory syndrome virus, N. Engl. J. Med. 350 (2004) 1731–1739.
[6] Y. Li, S. Duan, I.T. Yu, T.W. Wong, Multi-zone modeling of probable SARS virus transmission by airflow between flats in block E, amoy gardens, Indoor air 15 (2005) 96–111.
[7] C. Beggs, The airborne transmission of infection in hospital buildings: fact or fiction? Indoor Built Environ. 12 (2003) 9–18.
[8] J. Tang, Y. Li, I. Eames, P. Chan, G. Ridgway, Factors involved in the aerosol transmission of infection and control of ventilation in healthcare premises, J. Hosp. Infect. 64 (2006) 100–114.
[9] T.M.N. Nguyen, D. Ilef, S. Jarraud, L. Rouil, C. Campese, D. Che, et al., A community-wide outbreak of legionnaires disease linked to industrial cooling towers—how far can contaminated aerosols spread? J. Infect. Dis. 193 (2006) 102–111.
[10] H. Higson, R. Griffiths, C. Jones, D. Hall, Flow and dispersion around an isolated building, Atmos. Environ. 30 (1996) 2859–2870.
[11] B. Blocken, T. Stathopoulos, P. Saathoff, X. Wang, Numerical evaluation of pollutant dispersion in the built environment: comparisons between models and experiments, J. Wind Eng. Ind. Aerodyn. 96 (2008) 1817–1831.
[12] I. Mavroidis, R. Griffiths, D. Hall, Field and wind tunnel investigations of plume dispersion around single surface obstacles, Atmos. Environ. 37 (2003) 2903–2918.
[13] J.M. Santos, N.C. Reis Jr., E.V. Goulart, I. Mavroidis, Numerical simulation of flow and dispersion around an isolated cubical building: the effect of the atmospheric stratification, Atmos. Environ. 43 (2009) 5484–5492.
[14] H. Qian, Y. Li, P.V. Nielsen, X. Huang, Spatial distribution of infection risk of SARS transmission in a hospital ward, Build. Environ. 44 (2009) 1651–1658.
[15] H. Qian, Y. Li, P.V. Nielsen, C.-E. Hyldgård, T.W. Wong, A. Chwang, Dispersion of exhaled droplet nuclei in a two-bed hospital ward with three different ventilation systems, Indoor air 16 (2006) 111–128.
[16] K. Schenkel, R. Amarosa, I. Mücke, Risk assessment guidelines for infectious diseases transmitted on aircraft, Eur. Centre Dis. Prev. Control (2009) 1–58.
[17] H. Qian, Y. Li, Removal of exhaled particles by ventilation and deposition in a multibed airborne infection isolation room, Indoor air 20 (2010) 284–297.
[18] J. Hang, Y. Li, R. Jin, The influence of human walking on the flow and airborne transmission in a six-bed isolation room: tracer gas simulation, Build. Environ. 77 (2014) 119–134.

[19] J. Hang, Y. Li, W. Ching, J. Wei, R. Jin, L. Liu, et al., Potential airborne transmission between two isolation cubicles through a shared anteroom, Build. Environ. 89 (2015) 264–278.
[20] W. Liu, S. Mazumdar, Z. Zhang, S.B. Poussou, J. Liu, C.-H. Lin, et al., State-of-the-art methods for studying air distributions in commercial airliner cabins, Build. Environ. 47 (2012) 5–12.
[21] J. Niu, T.C. Tung, On-site quantification of re-entry ratio of ventilation exhausts in multi-family residential buildings and implications, Indoor air 18 (2008) 12–26.
[22] N.P. Gao, J.L. Niu, M. Perino, P. Heiselberg, The airborne transmission of infection between flats in high-rise residential buildings: tracer gas simulation, Build. Environ. 43 (2008) 1805–1817.
[23] N.P. Gao, J.L. Niu, M. Perino, P. Heiselberg, The airborne transmission of infection between flats in high-rise residential buildings: particle simulation, Build. Environ. 44 (2009) 402–410.
[24] X.P. Liu, J.L. Niu, K.C.S. Kwok, J.H. Wang, B.Z. Li, Investigation of indoor air pollutant dispersion and cross-contamination around a typical high-rise residential building: wind tunnel tests, Build. Environ. 45 (2010) 1769–1778.
[25] X.P. Liu, J.L. Niu, K.C. Kwok, J.H. Wang, B.Z. Li, Local characteristics of cross-unit contamination around high-rise building due to wind effect: mean concentration and infection risk assessment, J. Hazard. Mater. 192 (2011) 160–167.
[26] Z. Ai, C. Mak, J. Niu, Numerical investigation of wind-induced airflow and interunit dispersion characteristics in multistory residential buildings, Indoor air 23 (2013) 417–429.
[27] C. Gorlé, J. Van Beeck, P. Rambaud, G. Van Tendeloo, CFD modelling of small particle dispersion: the influence of the turbulence kinetic energy in the atmospheric boundary layer, Atmos. Environ. 43 (2009) 673–681.
[28] Z. Ai, C. Mak, CFD simulation of flow and dispersion around an isolated building: effect of inhomogeneous ABL and near-wall treatment, Atmos. Environ. 77 (2013) 568–578.
[29] Z. Ai, C. Mak, Determination of single-sided ventilation rates in multistory buildings: evaluation of methods, Energy Build. 69 (2014) 292–300.
[30] F. Haghighat, H. Brohus, J. Rao, Modelling air infiltration due to wind fluctuations—A review, Build. Environ. 35 (2000) 377–385.
[31] A.K. Blomsterberg, A Model Correlating Air Tightness and Air Infiltration in Houses, Lawrence Berkeley Natl. Lab. 2011. LBNL Paper LBL-9625. Retrieved from: http://escholarship.org/uc/item/3nn5t5vf.
[32] B. Zhao, J. Wu, Numerical investigation of particle diffusion in a clean room, Indoor Built Environ. 14 (2005) 469–479.
[33] T.C. Tung, J. Niu, J. Burnett, K. Hung, Determination of ozone emission from a domestic air cleaner and decay parameters using environmental chamber tests, Indoor Built Environ. 14 (2005) 29–37.
[34] E. Nederhoff, J. Van de Vooren, A.U. Ten Cate, A practical tracer gas method to determine ventilation in greenhouses, J. Agric. Eng. Res. 31 (1985) 309–319.
[35] E. Van Ouverkerk, S. Pedersen, Application of the carbon dioxide mass balance method to evaluate ventilation rates in livestock buildings, Appl. carbon dioxide mass balance method Eval. Vent. rates Livest. Build. (1994) 516–529.
[36] H.G.J. Snell, F. Seipelt, H.F.A. Van den Weghe, Ventilation rates and gaseous emissions from naturally ventilated dairy houses, Biosyst. Eng. 86 (2003) 67–73.
[37] G. Sze To, C. Chao, Review and comparison between the Wells–Riley and dose-response approaches to risk assessment of infectious respiratory diseases, Indoor air 20 (2010) 2–16.
[38] S. Rudnick, D. Milton, Risk of indoor airborne infection transmission estimated from carbon dioxide concentration, Indoor air 13 (2003) 237–245.
[39] G. Sze To, Risk assessment of infectious respiratory disease transmission in indoor environments, 2010.
[40] K. Sirén, The protection ability of the building shell against sudden outdoor air contamination, Build. Environ. 28 (1993) 255–269.
[41] D.-L. Liu, W.W. Nazaroff, Particle penetration through building cracks, Aerosol Sci. Technol. 37 (2003) 565–573.
[42] T.C. Tung, C.Y. Chao, J. Burnett, A methodology to investigate the particulate penetration coefficient through building shell, Atmos. Environ. 33 (1999) 881–893.
[43] A.C. Lai, W.W. Nazaroff, Modeling indoor particle deposition from turbulent flow onto smooth surfaces, J. aerosol Sci. 31 (2000) 463–476.